AAPS PharmSciTech, Vol. 12, No. 1, March 2011 (© 2011)
DOI: 10.1208/s12249-011-9593-2

Research Article

Templated Ultrathin Polyelectrolyte Microreservoir for Delivery of Bovine Serum Albumin: Fabrication and Performance Evaluation

Girish K. Gupta,[1] Vikas Jain,[1] and Prabhat Ranjan Mishra[1,2]

Received 19 May 2009; accepted 19 January 2011; published online 1 February 2011

Abstract. The aim of the study was to develop ultrathin polyelectrolyte microreservoir (UPM) using two combinations of synthetic/synthetic (S/s; poly(allylamine hydrochloride) (PAH)/sodium poly (styrenesulfonate)) and synthetic/natural (S/n; PAH/sodium alginate) polyelectrolytes over spherical porous $CaCO_3$ core particles (CP) followed by core removal and to evaluate its biocompatibility and integrity of loaded model protein bovine serum albumin (BSA). A novel process for synthesis of CP was developed to obtain maximum yield of monodisperse vaterite (spherical) polymorph. The prepared UPM was characterized for surface morphology, layer-by-layer growth, pay load efficiency, integrity of BSA, as well as viability and cell adhesion using murine J 774 macrophages (Φ). *In vitro* release profile revealed that both S/s and S/n UPM were able to provide sufficient diffusion barrier to release protein at physiological pH. It has been observed that S/n UPM are fully biocompatible due to obvious reason of using natural polymer. In a separate experiment, the S/s UPM surface was modified with pluronic F-68 to tune biocompatibility which provides evidences for safety and tolerability of the S/s UPM as well. In nutshell, the proposed system could successfully be used for the delivery of proteins, and moreover, the system can be tailored to impart desired properties at any stage of layering especially in terms of drug release and to retain the integrity of proteins.

KEY WORDS: biocompatible; cell adhesion; electrostatic attraction; layer-by-layer (LBL) assembly; natural polyelectrolyte.

INTRODUCTION

Most of the colloidal polymeric systems based on synthetic and natural polyelectrolyte (PEs) has been investigated by layer-by-layer (LBL) self-assembly technique for microencapsulation (1–4) and controlled release of macromolecules using different templates with size ranging from nanometer to tens of microns, such as organic to colloidal particles, protein aggregates, biological cells, and drug nano- or microcrystal (5). A system has been prepared by the sequential deposition of the oppositely charged PEs using phenomenon of electrostatic interaction between each other (6). Most of the colloidal templates can be decomposed at conditions where polymeric matrix is stable, which leads to the formation of hollow PE capsules with defined size, shape, and shell thickness. Encapsulation of macromolecules, proteins, and other bio-therapeutics into developed systems is of great interest for pharmaceutics and biotechnology due to its capability to use such systems as micro- and nanocontainers for controlled drug delivery (7). Besides this, they behave as good adjuvant even for mucosal immunization or for DNA vaccination (8). The study mainly emphasized on the use of combination of natural and synthetic polymers, and better results have been investigated compared to synthetic combination of PEs.

It has been reported that the naturally occurring biopolymer, alginate, has a peculiar property to form a matrix gel, which could be exploited for encapsulation/delivery of a biomacromolecules (9,10). In the proposed systems, we have exploited the gel formation property of alginate and further to enhance the surface area for electrostatic interaction within the pores of core particles (CP) to improve the payload efficiency and to control the size of microreservoirs. This alginate has been well recognized for the formation of strong complexes with polycation like proteins, polypeptides, and synthetic polymers. Many reports have been published with regard to encapsulation of proteins from alginate matrices to have claimed that all loading techniques require a lot of material and time (11–13). Dupuy and Minnot (14) have also reported that when alginate gel was prepared using poly-L-lysine as coating material, it form large size of beads (>1 mm in diameter) and microbeads in the size range of 0.2 mm in diameter (12,15).

There are several reports which reveal fabrication of layer-by-layer self-assembly using combination of synthetic PEs. The suitability of this synthetic PEs is still questioned as far as compatibility to bio-environment is concerned

[1] Pharmaceutics Division, Central Drug Research Institute, CSIR, Chattar Manzil Palace, M.G. Marg, Lucknow, 226001, India.
[2] To whom correspondence should be addressed. (e-mail: mishrapr@hotmail.com)

(16). Therefore, there could be two-tier approaches to mimic the system with bio-environment: (a) replacing synthetic with natural PEs and/or (b) modifying surface chemistry of developed system with bio-friendly agent using covalent coupling (17), hydrophobic interaction or adsorption by electrostatic interaction (18). It has been understood that replacing synthetic PEs with natural will undoubtedly lead to more biocompatible system. The surface chemistry of developed system often leads to valuable information to understand its behavior in physiological milieu/bio-environment. Therefore, surface modification seems to be an important tool to achieve both spatial and temporal drug delivery.

However, the main concern of this work is to prepare perfectly spherical $CaCO_3$ CP by using modified precipitation technique. It has been hypothesized that spherical $CaCO_3$ CP will provide uniform surface area for PEs coating to achieve monodisperse population of ultrathin polyelectrolyte microreservoir (UPM). Subsequently, the proposed study relates to development of UPM in two combinations—synthetic/synthetic (S/s) and synthetic/natural (S/n) PEs templated on decomposable, biocompatible, and bio-friendly porous template of inorganic origin (preformed $CaCO_3$ CP). The developed UPM system has been loaded with bovine serum albumin (BSA) and investigated the effect of combination of synthetic and natural (S/s and S/n) PEs on applicability to deliver BSA. An attempt has also been made to improve biocompatibility by modifying the surface of UPM made of S/s combination of PEs using pluronic F-68 (PF-68). Any changes in cell adhesion upon surface modification will provide valuable information with regard to suitability of system to deliver BSA in a controlled and precise manner in physiological milieu.

MATERIALS AND METHODS

Materials

The sources of chemicals are as follows: poly(allylamine hydrochloride) (PAH; molecular weight (Mwt.) 70,000), sodium poly(styrenesulfonate) (PSS; Mwt. 70,000), and sodium alginate (SA; Sigma, USA), fluorescein isothiocyanate (FITC; Sigma, USA), calcium chloride dihydrates ($CaCl_2 \cdot 2\ H_2O$, Ultra Sigma), sodium carbonate (Na_2CO_3, proanalysis, Merck, Germany), BSA (Sigma), Bradford reagent for protein determination, sodium lauryl sulfate, pluronic F-68, and brilliant green (were obtained from Sigma, St. Louis, MO, USA).

For cell culture, Dulbecco's modified eagle medium (DMEM) with Glutamax, fetal calf serum (FCS), and antibiotic solution (penicillin/streptomycin) were purchased from Sigma (St. Louis, MO, USA). Trypan blue solution, Giemsa stain, and 3-[4, 5-dimethylthiazol-2-yl]-2, 5-diphenyltetrazolium bromide (MTT) were from Sigma (St. Louis, MO, USA). Twenty-four- and 96-well plates, for cell adhesion and cell viability studies, respectively, were from Greiner Bio-One (Germany). All materials were used without further purification. The water used in all experiments was prepared in a three-stage Millipore Milli-Q plus 185 purification systems and had a resistivity higher than 18.2 mΩ cm.

Preparation of Porous $CaCO_3$ Core Particles and LBL Fabrication by Polyelectrolyte

Porous and spherical $CaCO_3$ CP with a narrow size range was prepared by colloidal crystallization from supersaturated (relative to $CaCO_3$) solution as reported by Volodkin *et al.* (7) with slight modification. Briefly, 10 ml volume of equimolar solution (0.33 M) of calcium chloride dihydrate was added to equal volume of sodium carbonate containing 0.4% (*w*/*v*) of pluronic F-68 and thoroughly stirred for 1 min. The CP thus obtained was thoroughly washed with triple distilled water (TDW) followed by acetone and vacuum dried at 50°C.

Two combinations (S/s and S/n) of UPM were developed comprising PAH/PSS (F-1) and PAH/SA (F-2), respectively, by alternate layering on preformed spherical $CaCO_3$ CP. Briefly, 0.1% (*w*/*v*) solution of each PEs was prepared in 0.5 M NaCl. The pH of the solutions was adjusted to 6.5 by adding appropriate amount of HCl or NaOH. In each experiment, preformed $CaCO_3$ (1%, *w*/*v*) CP were alternately suspended in different PEs solutions under gentle stirring for 15 min followed by centrifugation at 4,000 rpm. Excess of PEs was removed by extensive washing with TDW before initiating the next coating step. The procedure was repeated till the five alternate layers of oppositely charged PEs with respective surface charge (either positive or negative) were obtained. Finally, the core was removed by suspending in 0.1 M HCl for 30 min as reported by Sukhorukov (5). The resultant UPM (F-1: $(PAH/PSS)_5$; F-2: $(PAH/SA)_5$) were washed three times in TDW and stored at 2–8°C suspended in TDW.

In a separate experiment, an attempt was made to modify the surface of fabricated UPM $(PAH/PSS)_5$-PAH by incubating with 0.1% (*w*/*v*) PF-68 for 30 min and subsequent washing with TDW. Finally, these UPM were stored at 2–8°C in TDW. This surface modification was carried out with a view to assess any improvement in biocompatibility of S/s UPM. To fabricate fluorescent-labeled UPM, the same procedure was used with a final coating of PAH-FITC as reported by Volodkin *et al.* (7).

Encapsulation of BSA into UPM

One-milliliter UPM suspension was centrifuged at 20,000 rpm for 10 min, and the supernatant was removed. The UPM pellet thus obtained was re-dispersed/incubated in 1 ml of BSA solution (2.5 mg/ml) for 2 h. After incubation, the UPM suspension was centrifuged and washed thoroughly, and the supernatant thus obtained was used to estimate free BSA by Bradford method as reported by Smith *et al.* (19). The material balance of BSA was checked with free BSA in the supernatant and that encapsulated in the UPM.

Physicochemical Characterization

X-ray Diffraction

Powder X-ray diffraction (XRD) pattern of $CaCO_3$ CP, prepared by both conventional and modified co-precipitation technique, was recorded using a Rigaku D/max-3A instrument

(monochromatic CuK radiation). Typically, the diffractogram was recorded in a 2θ range of 5–25°C.

Scanning Electron Microscopy

The morphology of the prepared $CaCO_3$ CP and UPM was examined by scanning electron microscopy (SEM). Samples were prepared by applying a drop of particle suspension to glass slide and then drying overnight. Then samples were sputtered with gold and measurements were conducted using a Gemini Leo VP 435 instrument at an operation voltage of 3 keV.

Electrophoretic Mobility

Electrophoretic mobility of $CaCO_3$ CP and UPM suspended in Milli-Q water was measured after every adsorption using a Malvern Zetasizer Nano ZS (Malvern 3000HS).

Confocal Laser Scanning Fluorescence Microscopy

Confocal laser scanning fluorescence microscopy (CLSM) was carried out using Bio-red confocal scanning systems (Bio-red, USA) mounted to a Bio-red Aristoplan and equipped with a ×60 objective with a numerical aperture of 1.4. The excitation wavelength was 488 nm.

Differential Scanning Calorimetry

Differential scanning calorimetry (DSC; Diamond DSC, Perkin-Elmer, Germany) was used to study thermal properties of the PF-68 and surface-modified UPM ($(PAH/PSS)_5$-PAH-PF-68). The endothermic event was monitored from 30°C to 190°C with a heating rate of 5°C/min. The transition behavior was recorded during the first heating.

BSA Content in UPM

The BSA content of UPM was determined by the method as described by Volodkin *et al*. (7) with slight modification. Two hundred microliters of BSA-loaded UPM was treated with 0.1 M NaOH (pH>12) by vortexing for 15 min. The sample was centrifuged at 10,000 rpm for 10 min, and BSA concentration in the supernatant was determined by the Bradford method as reported by Smith *et al*. (19). Each sample was assayed in triplicate.

***In Vitro* BSA Release Study**

For *in vitro* release study, the ultrasink condition was used as reported by Volodkin *et al*. (7) with slight modification. Briefly, BSA-loaded UPM (200 μl) was taken from stock and dispersed using a vortex in 1 ml PBS (10 mM, pH 7.4). The sample was maintained under horizontal agitation at 37°C. At different time intervals, the dispersion was centrifuged at 10,000 rpm for 5 min, and the supernatant was assayed for BSA. After each sampling, the medium was replaced with fresh buffer. It was also ensured that no extra tiny particles are left in the supernatant. The medium was replaced with 1 ml fresh buffer after each determination. The pH was also monitored at each time point during release in order to observe any release of acidic fragments due to possible degradation of PEs. The % drug release at each sampling point was compared by Mann–Whitney *U* test and analyzed using a Kruskal–Wallis test.

Integrity of Proteins

In order to ensure any changes in integrity of BSA during processing of formulation (UPM), gel electrophoresis was carried out. Briefly, 100 μl of BSA-loaded UPM was dissolved in an equal volume of 0.1 M NaOH solution and was poured in electrophoretic sample buffer (×4) containing sodium dodecyl sulfate (SDS) and a reducing agent (β-mercaptoethanol), loaded onto a vertical slab gel (10%), and subjected to electrophoresis at 40 mA. The BSA separated by this way was fixed and stained with Coomassie brilliant blue R 250 (0.1%, *w*/*v*) in water/acetic acid/methanol (50:10:40). The integrity of free BSA left after encapsulation in UPM was also checked. In a separate experiment, circular dichroic (CD) of pure BSA and BSA in formulation was carried out in the range of 250 to 200 nm measured with a Dichrograph Mark III Spectropolarimeter.

Determination of Cell Adhesion or Phagocytosis

Murine J774 macrophages (MΦ) were used to study cell adhesion/phagocytosis of various UPM formulations. Cells were cultured in DMEM–L-glutamine supplemented with 10% heat-inactivated FCS containing 0.1% antibiotic solution (penicillin/streptomycin) at 37°C and 5% CO_2. MΦ cells were washed, collected by centrifugation, and counted by Trypan blue exclusion. About 400 μl (2×10^5 cells) of suspension was added per well into 24-well plates and further incubated at 37°C, 5% CO_2 for 2 h, and washed with DMEM to remove non-adherent cells. Then, 500 μl DMEM medium containing approximately 20–30 μg UPM was added to each well and incubated for 2 h to allow cell adhesion. After incubation, medium was aspirated and the cells were washed with DMEM, fixed with methanol for 5 min, and stained with Giemsa (10%, *v*/*v*) for 20 min. Excess of dye was washed with water; slides were dried and observed by light microscopy. The number of UPM adhered over macrophages was visualized by light microscopy, counting approximately 200 macrophages per well. The results were expressed as the percentage of the macrophages taking up either one or more than one UPM. To differentiate uptake of UPM by cell adhesion or phagocytosis, similar experiments were carried out at 4°C (data not shown).

Cytotoxicity by MTT Assay

A colorimetric assay based on the use of the tetrazolium salt, MTT, was used to assess cytotoxicity of different UPM formulations on murine J 774 MΦ. Viable cells are able to reduce MTT to colored formazan serving as indirect measurement of cell viability (20). Macrophages (4×10^4 cells) were incubated in 96-well plates (Greiner Bio-One, Germany) for 2 to 3 h in complete medium, washed with DMEM–L-glutamine, and further incubated for 1 h with 10 and 100 μg/ml UPM (the concentration employed is based on equivalent amount of

1% (*w/v*) $CaCO_3$ CP used for fabrication of UPM) in triplicate. Incubation medium was withdrawn, cells were washed, and the MTT (0.5 mg/ml) solution in DMEM complete medium was added to each well and incubated for 4 h. The supernatant was discarded and formazan crystals were dissolved in an extraction solution (isopropyl alcohol/dimethyl sulfoxide 3:1) overnight at 37°C. Finally, the plates were read at 550–570 nm (L1) and 620–650 nm (L2) as reference on scanning multiwell spectrophotometer. The formazan solution absorbs light at 550–570 nm, and absorbance at 630–650 nm usually results from cell debris and well imperfections. Final optical density (OD) obtained from formazan formation can be calculated OD=L1−L2.

Percentage cell survival is expressed as:

$$(\text{Absorbance of treated wells}/\text{Absorbance of control wells}) \times 100\%$$

RESULTS

The BSA-loaded LBL assembly of two oppositely charged PEs at solid surfaces of inorganic origin was developed by alternate adsorption of the PEs on a charged substrate due to their electrostatic attraction and the complex formation, resulting in the defined macromolecular layers on the surfaces (21) and well illustrated as in Fig. 1 reported by Volodkin *et al.* (7). In a separate experiment, an attempt was made to modify the surface of fabricated UPM, $(PAH/PSS)_5$-PAH by incubating with 0.1% (*w/v*) PF-68. This surface modification was carried out with a view to assess any improvement in biocompatibility of S/s UPM.

Physicochemical Characterization

The powder XRD data reveal (Fig. 2a) that all polymorphic forms of the $CaCO_3$ have been obtained during fabrication of porous particles such as calcite (rhombohedral), aragonite (hexagonal), and vaterite (spherical) due to mutual transformation between them (7) using conventional method of co-precipitation of calcium chloride dihydrate and sodium carbonate. However, to our interest, vaterite polymorph having uniform and spherical morphology was desirable as it is anticipated to provide uniform and amplified surface area so as to obtain uniform coating of PEs and high payload of BSA.

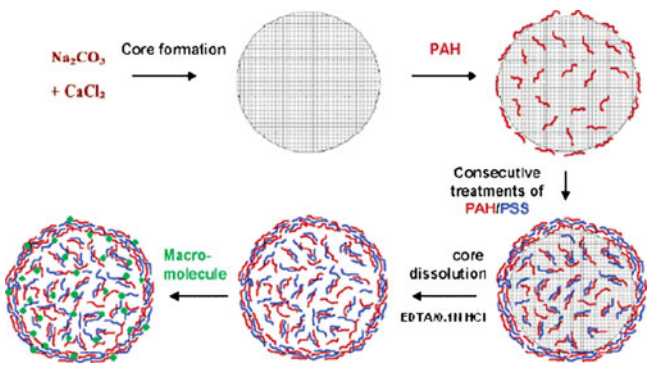

Fig. 1. Scheme of capsule fabrication and encapsulation of macromolecules into capsules (reported by Volodkin *et al.* (7))

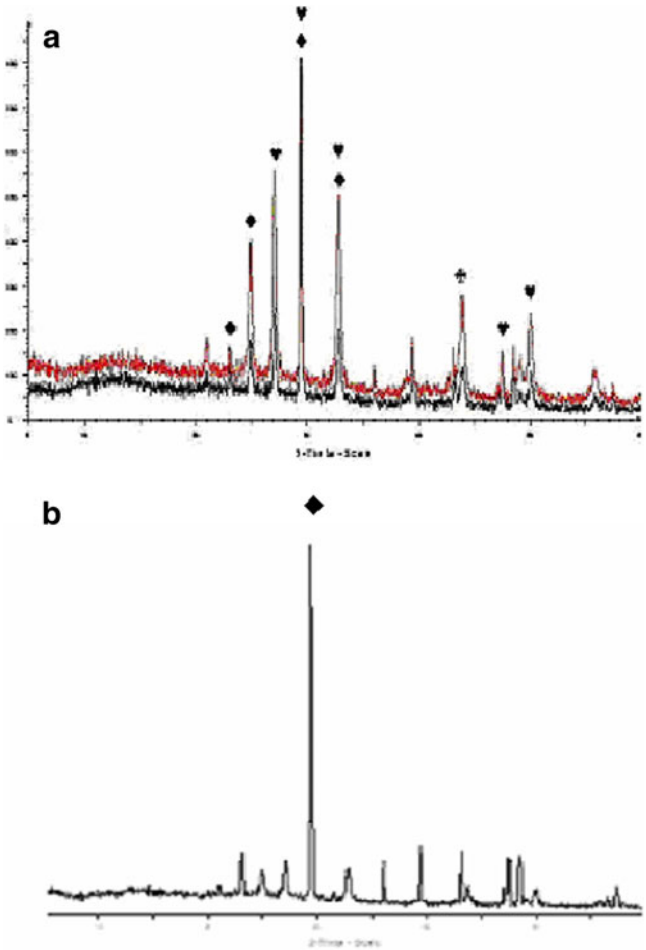

Fig. 2. XRD pattern of different polymorphs of porous $CaCO_3$ CP. **a** Core particle prepared by conventional method (co-precipitation of calcium chloride dihydrate and sodium carbonate); **b** core particle prepared by modified method (co-precipitation in presence of PF-68). *Black club suit* aragonite (*hexagonal*), *black heart suit* calcite (*rhombohedral*), *black diamond suit* vaterite (*spherical*)

Conventional procedure was modified by incorporating appropriate concentration of PF-68 during controlled co-precipitation that lead to the formation of vaterite (spherical) polymorph in abundance as shown in Fig. 2b. These polymorph was spherical, non-aggregated, and monodisperse as demonstrated by SEM (Fig. 3a). The striated surface of the fabricated UPM clearly indicates that the coating of PEs has occurred over the smoother porous CP as shown in Fig. 3b. The size distribution of $CaCO_3$ CP was found to be 3240 d.nm as determined by Malvern Zetasizer Nano ZS (Malvern 3000HS).

The electrostatic attraction is the driving force for the LBL assembly of oppositely charged PEs onto the $CaCO_3$ CP for encapsulation of BSA. Positively charged PAH was deposited as the first layer on the $CaCO_3$ particles because of the intrinsic negative ζ-potential on the $CaCO_3$ particle (>−20 mV) surface at a given pH. The next layer is negatively charged PSS, and the process is repeated until desired number of layers of PAH/PSS was obtained and the same was repeated with (PAH/SA) combination. Subsequent adsorption of polycation and polyanion leads to reversal of ζ-potential in accordance with the charge of the PEs as

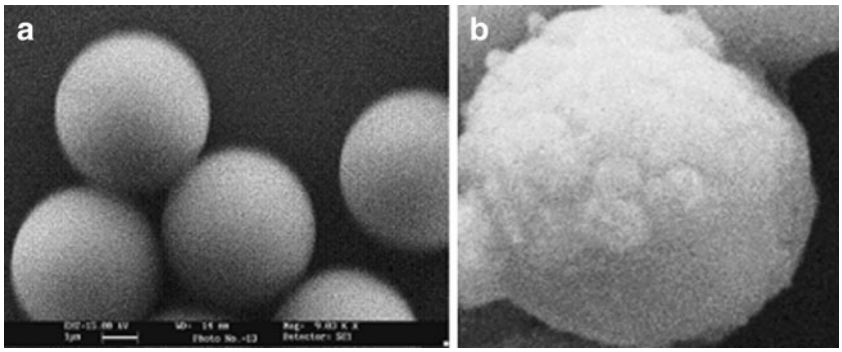

Fig. 3. **a** Scanning electron microscopy of bare $CaCO_3$ CP. The surface of $CaCO_3$ CP as observed is porous in texture. **b** Coated UPM capsule. The slight rough surface is due to coating of PEs. *Scale bar*, 1 μm

illustrated in Fig. 4. The confocal laser scanning picture has been represented in Fig. 5, which depicts such an increase in fluorescence after adsorption of layers of fluorescently labeled PAH, and moreover, it confirms the multilayer growth.

The surface modification of UPM was carried out with adsorption of PF-68 at the fabricated surface. Electrophoretic examination of the capsules showed a marked decrease in the surface charge (from 20.6±3.2 to 6.8±2.1 mV). This clearly indicates that surface modification of the shells has occurred and existence of a small overall positive charge even after adsorption of neutral PF-68, which contributes to the measured surface charge. Additionally, the surface-modified UPM showed two marked endothermic peaks at 100°C and 180°C by differential scanning calorimeter (Fig. 6), when endothermic event was monitored from 30°C to 190°C with a heating rate of 5°C/min. A sharp endothermic peak of pure PF-68 was obtained at 58.6°C, corresponding to its melting temperature. The entrapment efficiency was found to be approximately 78±4.6% and 74±2.1% for $(PAH/PSS)_5$ and $(PAH/SA)_5$, respectively. The *in vitro* release profile of BSA-loaded capsules prepared by LBL technique using $(PAH/PSS)_5$-PAH and $(PAH/SA)_5$ was investigated in PBS (pH=7.4). The release from formulation $(PAH/SA)_5$ was 43.63±4.8% whereas from formulation $(PAH/PSS)_5$ the amount of BSA released was 44±5.76% after 24 h. However, after 24 h, the release from both formulations has steadily slowed down (shown in Fig. 7). There was no significant difference ($p<0.05$) in the release profile of both the formulations.

Integrity of Proteins

SDS–polyacrylamide gel electrophoresis (PAGE) analysis of pure BSA, free, and entrapped BSA in the formulations was undertaken using the method described by Laemmli (22) with slight modifications. PAGE followed by Coomassie blue staining revealed identical bands for the released BSA from formulation after treatment with 0.1 M NaOH to pure BSA (Fig. 8a). The circular dichroic of pure BSA and BSA in formulation showed similarity as negative bands for both were in the range of 225–248 nm which indicates that the secondary structure is maintained.

Determination of Cell Adhesion

The UPM comprised of synthetic PE having positive charge ($(PAH/PSS)_5$-PAH) as outermost layer adhered

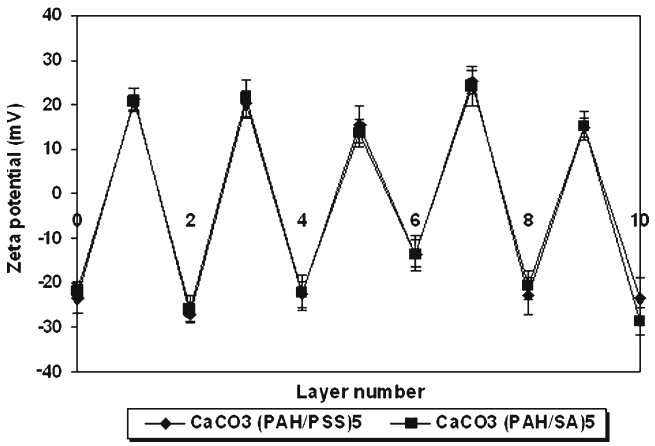

Fig. 4. Demonstration of layer-by-layer growth of UPM as a function of ζ-potential. The ζ-potential was measured in Milli-Q water at each adsorption step. Layer 0 indicates ζ-potential of bare $CaCO_3$ particles. The data represented as average value of three separate experiments

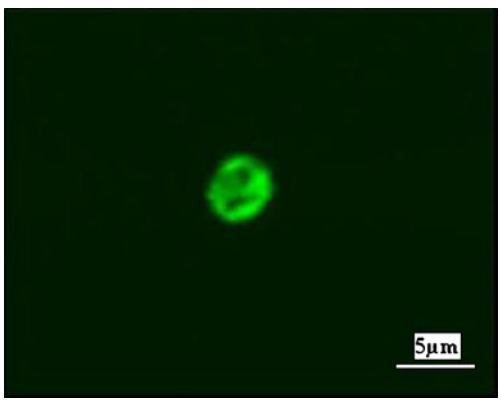

Fig. 5. Confocal laser scanning microphotograph of PAH-FITC-tagged UPM (magnification, ×60). The fluorescence on the surface indicates uniform coating of PEs as well as multilayer growth. The appearance of fluorescence at the interior reveals that PAH-FITC extends itself into the pores of $CaCO_3$ core and participates in matrix formation

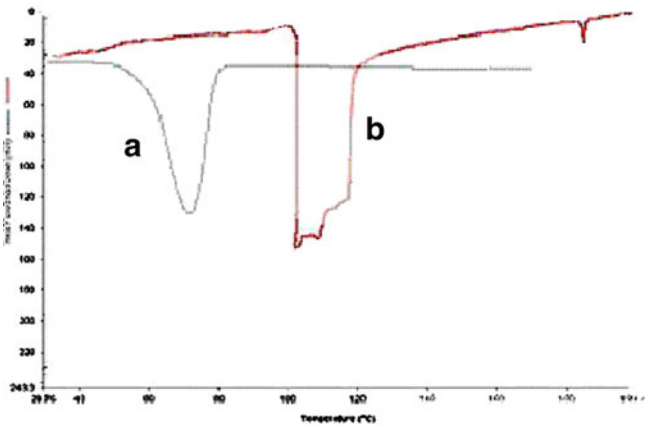

Fig. 6. Differential scanning thermogram of PF 68 and PF 68-coated UPM. Endothermic event of **a** PF-68 and **b** PF-68 coated UPM, respectively. The endothermic event was monitored from 30°C to 190°C with a heating rate of 5°C/min. The transition behavior was recorded during the first heating

immediately, and more than 90% of particles were adhered after 2 h of incubation. Each cell was found to have around 15–20 particles adhered to them. In contrast, when PSS was replaced by SA as in case of $(PAH/SA)_5$ PAH, the non-specific adherence was reduced to 63%. The % cell adhesion by different formulations has been shown in Fig. 9, and a typical photomicrograph is given in Fig. 10. Our data suggest that the physiologic distribution of UPM could be modified substantially by simply replacing the synthetic PEs with a natural one. Surface modification of UPM with PF-68 ($(PAH/PSS)_5$-PAH-PF68) efficiently reduced cell adhesion by MΦ, and there was no immediate adhesion, and after 2 h of incubation, about 50–55% of the cells were found to have 3–4 particles adhered to them. It is interesting to note that degree of cell adhesion of $(PAH/PSS)_5$-PAH-PF68 was not increased even when incubated for up to 3 days (data not shown) at either 4°C or 37°C.

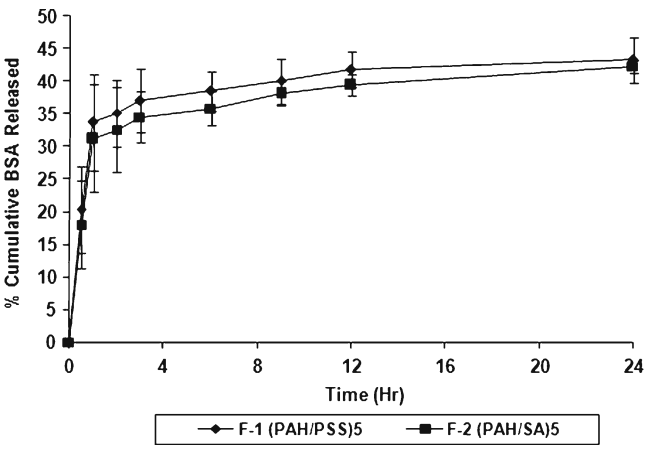

Fig. 7. Cumulative release profile of BSA from different UPN formulations in PBS pH 7.4. The *error bars* indicates ± SD of three set of experiments (n=3). The release experiment was performed maintaining ultrasink condition by replacing complete buffer at each time point. It is noted that the pH at each time point was not altered indicating stability of PEs employed

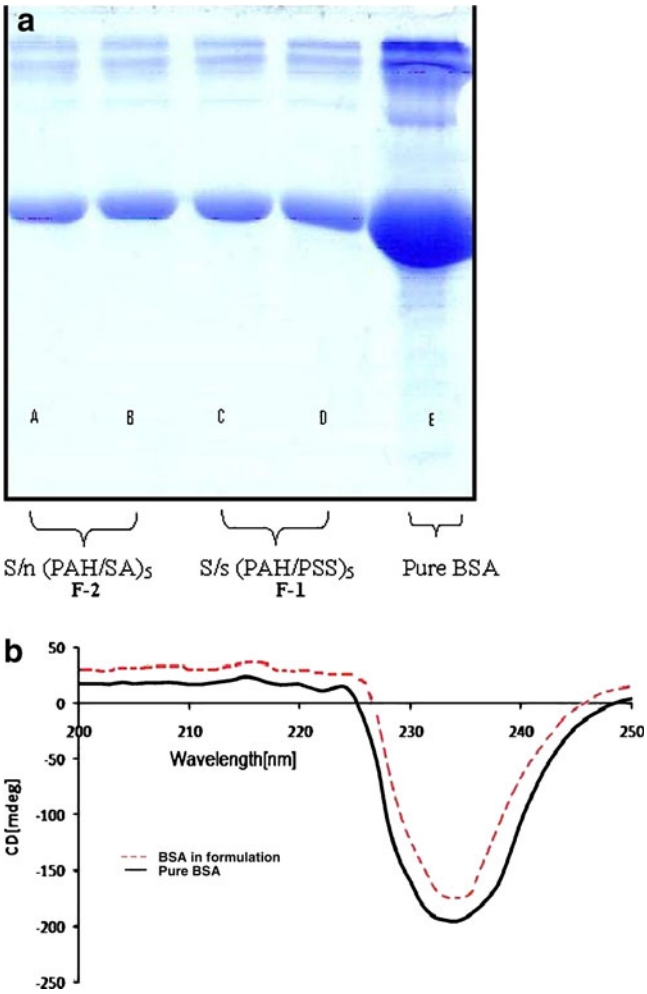

Fig. 8. **a** Coomassie R-250 stained electrophoretic gel picture of BSA released from different UPM formulations $(PAH/SA)_5$ and $(PAH/PSS)_5$ containing equimolar concentration of pure BSA. *A*, *B* Entrapped and free BSA for S/n$(PAH/SA)_5$, respectively; *C*, *D* entrapped and free BSA for S/s $(PAH/PSS)_5$, respectively; *E* pure BSA. One hundred microliters of UPM suspension dissolved in 0.1 M NaOH poured in electrophoretic sample buffer (×4) containing SDS loaded onto a vertical slab and subjected to electrophoresis at 40 mA. **b** Circular dichroism spectra of BSA released from UPM formulation. Pure BSA (*black line*) and BSA in microreservoir $(PAH/PSS)_5$ (*red dotted line*)

Cytotoxicity by MTT Assay

MTT tetrazolium salt assay revealed dose-dependent cytotoxicity of (S/s) and (S/n) UPM on cell viability using macrophage cell line (J 774 MΦ) considering a 100% viability in plain cells without UPM. In our studies, a composition comprising synthetic and natural polyelectrolyte (i.e., S/n) was found to be less toxic as the viability was 76.1±12.2% and 43.4±2.3% at two dose levels, i.e., 10 and 100 μg/ml (with respect to $CaCO_3$ as core), respectively, while the cell viability of S/s was reduced to 39.3±8.3% at 10 μg/ml of UPM concentration. However, there was no significant difference in surface ζ-potential between two formulations as S/s and S/n showed +19.2±1.7 and +20.6±1.2 mV. Upon surface modification of S/s UPM with PF-68 ($(PAH/PSS)_5$-PAH-PF68), the cell viability was dramatically improved to

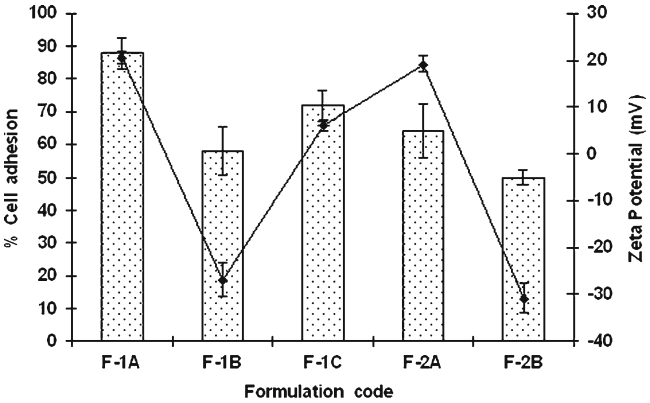

Fig. 9. Cell adhesion study of various UPM formulations on J 774 MΦ. The data represents total number of cells having one or more than one adhered UPM particles after incubation for 2 h at 37°C (*left axis in bars*). Effect of surface ζ-potential on adhesion of different UPM formulations has been shown in (*right axis in line*). *F-1* $(PAH/PSS)_5$-PAH, *F-2* $(PAH/PSS)_5$-PAH-PF68, *F-3* $(PAH/PSS)_5$, *F-4* $(PAH/SA)_5$ PAH, *F-5* $(PAH/SA)_5$. The *error bars* indicate ± SD of three set of experiments (n=3)

76.1±5.0% with positive ζ-potential (+6.2±1.2 mV) as illustrated in Fig. 11.

DISCUSSION

The encapsulation technique usually involves solubilization of polymers in organic solvent, which leads to high encapsulation efficiency but low drug loading capacity. To overcome the above impediment, UPM was developed through LBL adsorption of PEs, although most of the used PEs may or may not be bio-absorbable, biocompatible, and biodegradable in the physiological environment (16). In the present study, the multilayer films were comprised of five pairs of PEs either in synthetic or natural in origin. The technique was usually performed in the aqueous solution at room temperature, and thus, it was suitable for encapsulating therapeutic proteins or other bio-therapeutics with poor stability. Among the decomposable cores porous $CaCO_3$ drives interest due to its wide industrial, technological, and drug delivery applications (23–26). The controlled crystallization of $CaCO_3$ resulting in the formation of uniform, homogenous, and non-aggregated CP. This effect could be ascribed to adsorption of PF-68 on the surface and thus preventing aggregation and crystallization. It has also been observed that the shape and morphology of $CaCO_3$ CP were remained unaltered during storage period of at least 3 months (data not shown). The electrostatic attraction is the driving force for the LBL assembly of oppositely charged PEs onto the $CaCO_3$ CP. Usually this alternation indicated multilayer growth; however, few cases are reported (27,28), where desorption of the PEs layer by the oppositely charged PEs lead to switch off ζ-potential. The proof of layers deposition can be given only by studies of the growth of the adsorbed material amount. The multilayer growth can also be adjudged by using the FITC-tagged polymer to be coated as last layering. It has been reported by Antipov *et al.* (29) that, if a PEs labeled with a fluorescence moiety are used as the layer constituent, its adsorption can easily be detected by fluorescence, which will also indicate multilayer growth. Moreover, it exhibits some fluorescence at the interior when observed by CLSM, which could be due to the fact that some of FITC-PAH might have penetrated into $CaCO_3$ core matrix. This study also suggests that the prepared $CaCO_3$ core is porous in nature and the UPM has acquired matrix type structure without precipitation of PEs on the surface (7). The step of surface modification of the PAH/PSS-PAH-multilayered shells with PF-68 involves adsorption or interlayer hydrophobic interaction between them which imparts additional stability and biocompatibility. It is well-known that assembling layer by layer along with closely packed hydrophilic, hydrophobic chains followed by exposure to aqueous solution provides hydrophilic brushes on the surface (30). The higher transition temperatures as observed in DSC thermograms obtained for cross-linked UPM might be attributed to increased inter- and intramolecular interaction between the hydrophilic–hydrophobic chains in presence of water (31).

The high surface area and the pores in CP have opened the perspective for encapsulation and spontaneous accumulation of biomacromolecules such as BSA via physical adsorption and/or pore diffusion. It is well-known that the encapsulation could be achieved after the UPM are obtained and the material of interest could be driven into or generated *in situ* within the capsules using physiochemical forces like pH/concentration/ionic/polarity gradient, or complexation,

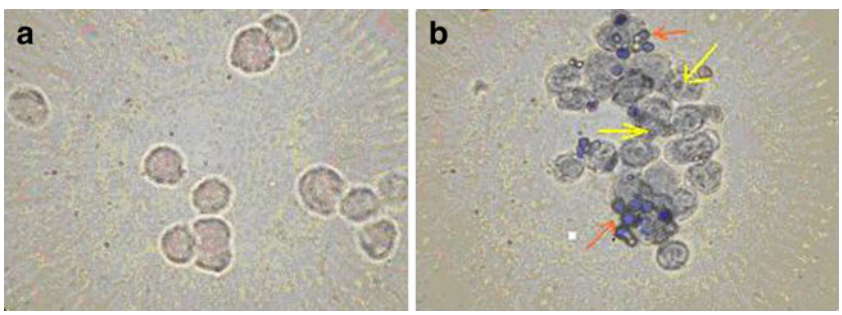

Fig. 10. Normal phase contrast microscopy of **a** plain J 774 MΦ and **b** adhered S/n $(PAH/SA)_5$ UPM (×100). The culture medium used was DMEM medium, and the study was conducted for 2 h. It has been observed that not more than 50% of J 774 MΦ were found adhered with UPM in case of $(PAH/SA)_5$ while more than 10 UPM per cell were found adhered in case of S/s $(PAH/PSS)_5$-PAH (figure not shown). The *arrow* indicates adhesion/phagocytosis of UPM capsules

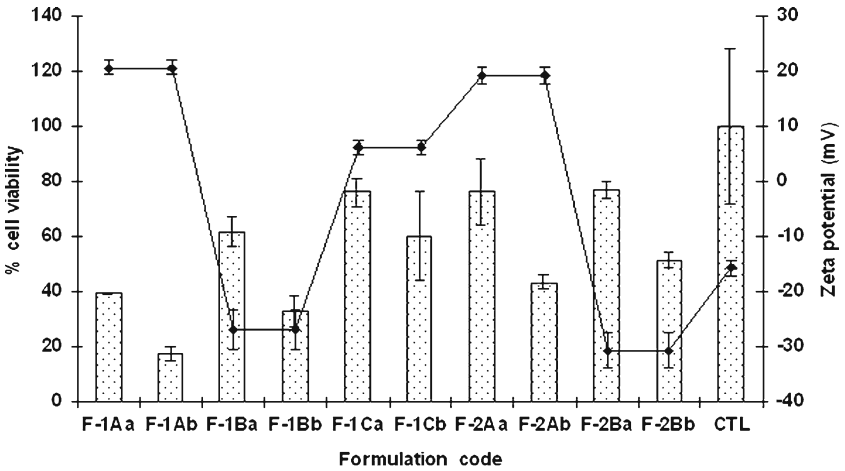

Fig. 11. Cell viability study of various UPM formulations on J 774 MΦ at two different concentrations (A=10 μg/ml; B=100 μg/ml) by MTT assay (*left axis in bars*). The concentration employed is based on equivalent amount of 1% (*w*/*v*) $CaCO_3$ used for fabrication of UPM. Effect of surface ζ-potential on cell viability of different UPM formulations has been shown in (*right axis in line*). *F-1* $(PAH/PSS)_5$-PAH, *F-2* $(PAH/PSS)_5$, *F-3* $(PAH/PSS)_5$-PAH-PF68, *F-4* $(PAH/SA)_5$-PAH, *F-5* $(PAH/SA)_5$, *CTL* J 774 MΦ. The *error bars* indicate ± SD of three set of experiments (n=3)

etc. This phenomenon is due to strong electrostatic interactions between free surface charge of polyelectrolyte matrix inside the capsules and the surface charge of amino acids of proteins BSA. The release profile of formulations exhibited sustained release over a period of 24 h. To rule out the possibility of any kind of polymeric degradation, the pH of the medium was checked at every time point along with released sample. It was interesting to note that the pH of the release media was not altered as in the case of other polymeric excipients such as PLL, PLA, PLGA, etc. (32–34). It suggests that the employed PEs could be used for delivering proteins and acid labile compounds and able to maintain the structural integrity of the macromolecules in the release media while the conventional polymers like PLA or PLGA are not suitable for delivering therapeutic proteins.

Structural integrity of released BSA was confirmed using Coomassie blue staining as demonstrated in Fig. 8a. Moreover, the secondary structure of BSA was confirmed using CD spectra (Fig. 8b). These data revealed patterned and identical bands for the released BSA from different formulations when compared to standard BSA. There were no additional bands which are nullifying the presence of any (molecular weight 66 kDa) fragments produced by proteolysis. However, the data suggested that the structural integrity of BSA is thoroughly maintained throughout the processing of formulation.

Cell adhesion of (S/s) and (S/n) UPM was investigated using macrophage cell line J 774 MΦ. It has been observed that the degree of cell adhesion is affected by both surface charge and type of PE (synthetic or natural) disguised as outermost layer. However, the role of surface charge is controversial (35,36) as there are other particle characteristics such as particles hydrophobicity and size influencing the cell adhesion (37). The % cell adhesion by different formulations has been shown in Fig. 9, and a typical photomicrograph is given in Fig. 10. The data also suggest that the UPM comprised of natural PE (SA) have capacity to inhibit cell adhesion compared to synthetic ones. Moreover, surface modification of UPM with PF-68 can reduce non-specific uptake by J774 MΦ even if UPM comprised of synthetic PEs having outermost positive charge. Thus, inhibition of phagocytosis by $(PAH/PSS)_5$-PAH-PF68 could be attributed to hydrophilicity imparted by PF-68. This observation is supported by the fact that bacteria being more hydrophobic than phagocytes are readily engulfed (38).

The cellular biocompatibility of developed formulations was assessed using MTT tetrazolium salt assay. Metabolic active cells have the capacity to transform tetrazolium salt into formazan (20), providing evidence of the integrity and activity of the mitochondrial enzymes and cell viability (38). It has been known through literature that toxicity at cellular level could be derived either from type of polyelectrolyte or surface charge. Our data suggest that S/s UPM is more toxic than S/n combination. This is in conformity with the previous observation that natural polyelectrolytes are more biocompatible than synthetic one. However, it is interesting to note that the surface ζ-potential of both the formulations is nearly same which is in contrary to previous observations. This result provides evidences that the biocompatibility is being affected irrespective of ζ-potential. In our study, it is only the type of polyelectrolyte which is playing a pivotal role in affecting cellular biocompatibility. However, upon surface modification of S/s UPM with PF-68, the cell viability was significantly improved and was equivalent to S/n UPM formulation which could be attributed to surface hydrophilicity imparted by PF-68. These data suggest that the properties of S/s formulation could also be enjoyed subsequent to surface modification. We are of the opinion that this value will exceed during *in vivo* intervention, since live cells has clearance mechanisms that withdraw potentially toxic degradation products from PEs. However, these values do not indicate cell mortality but mitochondrial damage that may be due to the interaction between capsules and the cells. In addition, the population of microcapsules placed in contact with cells was really high enough to observe the maximum toxic effect. Impetus to these data, it is obvious that the proposed system can potentially be used for controlled

delivery of therapeutic proteins with high payload. However, the system is suitable for both small and macromolecules and therefore could be applied in variety of pathological conditions. Interestingly, the system may be administered through invasive and non-invasive routes, e.g., oral, pulmonary, nasal, ocular, and as injectables.

CONCLUSION

The fabrication of microreservoir using combination of synthetic and natural PEs seems to be promising carrier for controlled delivery of therapeutic proteins without affecting its integrity. The surface modification of S/s UPM with PF-68 has demonstrated that biocompatibility could be successfully achieved even with synthetic PEs. Our data suggest that the repellant behavior of $(PAH/PSS)_5$-PAH-PF68 may be maintained for time period that might be sufficient to significantly alter the biodistribution and enhance their circulation time *in vivo*. Further studies are still underway to obtain suitable combination of natural PEs to get better targeting efficacy of the system.

ACKNOWLEDGMENTS

Financial assistance to Dr. P.R. Mishra through CSIR XI Network project (NWP 0035) on "Nanomaterials and Nanodevices for applications in Health and diseases" is gratefully acknowledged. Girish K Gupta and V. Jain are thankful to Indian Council of Medical Research and Council of Scientific and Industrial Research, New-Delhi, India for providing Senior Research Fellowships and Research Associate fellowship, respectively. Prof. S.C. Lakhotia, Department of Zoology, Banaras Hindu University, Varanasi, India is gratefully acknowledged for providing Confocal Laser Scanning Microphotography facility. The CDRI communication no. is 7409.

REFERENCES

1. Gao CY, Donath E, Mohwald H, Shen JC. Spontaneous deposition of water-soluble substances into microcapsules: phenomenon, mechanism and application. Angew Chem Int Ed. 2002;41:3789–93.
2. Sukhorukov GB, Donath E, Moya S, Susha A, Voigt A, Hartmann J, *et al.* Microencapsulation by means of step-wise adsorption of polyelectrolytes. J Microencapsul. 2000;17:177–85.
3. Lvov Y, Antipov AA, Mamedov A, Mohwald H. Urease encapsulation in nanoorganized microshells. Nano Lett. 2001;1: 125–8.
4. Dahne L, Leporatti S, Donath E, Mohwald H. Fabrication of micro reaction cages with tailored properties. J Am Chem Soc. 2001;123:5431–6.
5. Sukhorukov G. Designed nano-engineered polymer films on colloidal particles and capsules. In: Mobius D, Miller R, editors. Novel methods to study interfacial layers. Amsterdam: Elsevier Science; 2001. p. 383–414.
6. Decher G, Hong JD, Schimtt J. Buildup of ultrathin multilayer films by a self-assembly process: III. Consecutively alternating adsorption of anionic and cationic polyelectrolytes on charged surfaces. Thin Solid Films. 1992;210(1–2):831–5.
7. Volodkin DV, Petrov AI, Prevot M, Sukhorukov GB. Matrix polyelectrolyte microcapsules: new system for macromolecule encapsulation. Langmuir. 2004;20(8):3398–406.
8. Shchukin DG, Patel AA, Sukhorukov GB, Lvov YM. Nanoassembly of biodegradable microcapsules for DNA encasing. J Am Chem Soc. 2004;126:3374–5.
9. Pommersheim R, Schrezenmeir J, Voigt W. Immobilization of enzymes by multilayer microcapsules. Macromol Chem Phys. 1994;195:1557–67.
10. Gombotz WR, Wee SF. Protein release from alginate matrices. Adv Drug Deliv Rev. 1998;31:267–85.
11. Singh ON, Burgess DJ. Characterization of albumin–alginic acid complex coacervation. J Pharm Pharmacol. 1989;41:670–3.
12. Ku C, Dixit V, Shaw W, Gitnick G. *In vitro* slow release profile of endothelial cell growth factor immobilized within calcium alginate microbeads. Artif Cells Blood Substit Immobil Biotechnol. 1995;23:143–51.
13. Vandenberg GW, De La Noue JJ. Evaluation of protein release from chitosan–alginate microcapsules produced using external or internal gelation. J Microencapsul. 2001;18:433–41.
14. Dupuy B, Minnot AP. FT-IR of membranes made with alginate/polylysine complexes—variations with the mannuronic or gulur-onic content of the polysaccharides. Artif Cells Blood Substit Immobil Biotechnol. 1994;22:71–82.
15. Martisen A, Skjak-Braek G, Smidsrod O. Alginate as immobilization material: I. Correlation between chemical and physical properties of alginate gel beads. Biotechnol Bioeng. 1989;33: 79–89.
16. Sukhorukov GB, Mohwald H. Multifunctional cargo systems for biotechnology. Trends Biotechnol. 2007;25(3):93–8.
17. Zahr AS, De Villiers M, Pishko MV. Encapsulation of drug nanoparticles in self-assembled macromolecular nanoshells. Langmuir. 2005;21:403–10.
18. Khopade AJ, Caruso F. Surface modification of polyelectrolyte multilayered-coated particles for biological application. Langmuir. 2003;19:6219–25.
19. Smith PK, Krohn RI, Hermanson GT, Mallia AK, Gartner FH, Provenzano MD, *et al.* Measurement of protein using bicinchoninic acid. Anal Biochem. 1985;150:76–85.
20. Hansen MB, Nielsen SE, Berg K. Re-examination and further development of a precise and rapid dye method for measuring cell growth/cell kill. J Immunol Meth. 1989;119:203–10.
21. Decher G. Fuzzy nanoassemblies: towards layered polymeric multicomposite. Science. 1997;277:1232–7.
22. Laemmli UK. Cleavage of structural proteins during the assembly of bacteriophage T4. Nature. 1970;277:680–5.
23. Caruso F, Caruso RA, Mohwald H. Nanoengineering of inorganic and hybrid hollow spheres by colloidal templating. Science. 1998;282:1111–4.
24. Ye S, Wang C, Liu X, Tong Z. Deposition temperature effect on release rate of indomethacin microcrystals from microcapsules of layer-by-layer assembled chitosan to alginate multilayer films. J Control Release. 2005;106:319–28.
25. Donath E, Moya S, Neu B, Sukhorukov GB, Georgieva R, Voigt A, *et al.* Hollow polymer shells from biological templates: fabrication to potential applications. Chem Eur J. 2002;8:5481–5.
26. An ZH, Lu G, Mohwald H, Li JB. Self assembly of human serum albumin and L-alpha-dimyristoylphosphatidic acid (DMPA) microcapsules for controlled drug release. Chem Eur J. 2004;10: 5848–52.
27. Hoogeveen NG, Stuart MAC, Fleer GJ, Boher MR. Formation and stability of multilayers of polyelectrolytes. Langmuir. 1996; 12:3675–81.
28. Dubas ST, Schlenoff JB. Polyelectrolyte multilayers containing a weak polyacid: construction and deconstruction. Macromolecules. 2001;34:3736–40.
29. Antipov AA, Shchukin L, Fedutik Y, Petrov AI, Sukhorukov GB, Mohwald H, *et al.* Carbonate microparticles for hollow polyelectrolyte capsules fabrication. Colloids Surf, A Physicochem Eng Asp. 2003;224:175–83.
30. Winger TM, Ludovice PJ, Chaikof EL. Formation and stability of complex membrane-mimetic monolayers on solid supports. Langmuir. 1999;15:3866–74.
31. Lee JW, Park JK, Lee JH. Thermo sensitive permeation from side-chain crystalline ionomers. J Polym Sci, B, Polym Phys. 2000;38:823–30.
32. Yan C, Resau JH, Heweston J, West M, Rill WL, Kende M, *et al.* Characterization and morphological analysis of protein loaded

poly (lactide-co-glycolide) microparticles prepared by water-in-oil-in-water emulsion technique. J Control Release. 1994;32:231–41.
33. Gander B, Thomasin C, Merkle HP, Men Y, Corradin G. Pulsed tetanus toxoids release from PLA-microspheres to its relevance for immunogenicity in mice. Proc Int Symp Control Release Bioact Mater. 1993;20:65–6.
34. Schwendeman SP, Costantino HR, Gupta RK, Tobio M, Chang AC, Alonso MJ, *et al*. Strategies for stabilizing tetanus toxoid towards the development of a single-dose tetanus vaccine. In: Brown F, editor. New approaches to stabilization of vaccines potency. Dev Biol Stand, 57. Basel: Karger; 1996. p. 293–306.
35. Tabata Y, Ikada Y. Effect of size and surface charge of polymer microspheres on their phagocytosis by macrophage. Biomaterials. 1988;9:356–62.
36. Torche AM, Corre L, Albina P, Jestin EA, Verge R. PLGA microspheres phagocytosis by pig alveolar macrophages: influence of poly (vinyl alcohol) concentration, nature of loaded-protein and copolymer nature. J Drug Target. 2000;7:343–54.
37. Muller RH, Ruhl D, Paulke BR. Influence of fluorescent labeling of polystyrene particles on phagocytic uptake surface hydrophobicity and plasma protein adsorption. Pharm Res. 1997;14:18–24.
38. McEvoy L, Williamson P, Schlegel RA. Membrane phospholipid asymmetry as a determinant of erythrocyte recognition by macrophages. Proc Natl Acad Sci USA. 1986;83:3311–5.